Available online at www.sciencedirect.com
SCIENCE DIRECT
ELSEVIER
Virology 345 (2006) 258 – 269
VIROLOGY
www.elsevier.com/locate/yviro

Lack of WHV integration nearby N-*myc*2 and in the downstream *b3n* and *win* loci in a considerable fraction of liver tumors with activated N-*myc*2 from naturally infected wild woodchucks

Roberto Bruni [a], Ivano Conti [a], Umbertina Villano [a], Roberto Giuseppetti [a], Giampiero Palmieri [b], Maria Rapicetta [a,*]

[a] *Department of Infectious, Parasitic and Immunomediated Diseases, Viral Hepatitis Unit, Istituto Superiore di Sanità, Viale Regina Elena 299, 00161 Rome, Italy*
[b] *Department of Biopathology, Section of Pathological Anatomy, School of Medicine, Policlinico Tor Vergata, University of Rome "Tor Vergata", Viale Oxford 81, 00133 Rome, Italy*

Received 29 July 2005; returned to author for revision 8 September 2005; accepted 30 September 2005
Available online 3 November 2005

Abstract

In liver tumors induced by chronic WHV infection in the WHV/woodchuck model of HBV infection, activation of genes of the *myc* family by WHV insertion has been well documented. Several studies have shown that N-*myc*2 is by far the most frequently involved, and in most cases, its transcriptional activation is due to WHV insertion nearby the gene. N-*myc*2 has been shown to be also activated by WHV insertion in two downstream loci, *b3n* and *win*. Although the extent of insertion in these latter loci in woodchuck tumors has not been investigated, their discovery has led to the notion that therein WHV insertion accounts for N-*myc*2 activation in the remaining tumors expressing the proto-oncogene in absence of any detectable alteration nearby the gene, a notion remained unproved and not further investigated yet.

In the majority of cases, the above observations were derived from tumors developed in colony born laboratory bred woodchucks experimentally infected with standardized viral inocula, mostly of the same lineage.

In the present work, we investigated a survey of liver tumors naturally developed in wild woodchucks with naturally acquired chronic WHV infection. Tumors had histological features of well to moderately differentiated HCCs. In most animals, multiple tumor nodules were observed; in the great majority of cases, they were shown to be independent tumors because their WHV integration patterns were not clonally related. 53 independent tumors were investigated for N-*myc* activation and WHV integration nearby N-*myc* genes and in the *b3n* and *win* loci.

Comparison of our results with data from previous studies revealed that, in tumors from naturally infected wild woodchucks, the frequency of WHV integration nearby N-*myc*2 has a tendency to be lower and, in addition, N-*myc*2 activation is due to WHV integration nearby the gene significantly less frequently than in tumors from experimentally infected colony born animals (12/28, 43% vs. 15/20, 75%, $P = 0.0397$). These findings are likely related to the less uniform conditions as to infecting virus and host genetic background in naturally infected wild woodchucks with respect to experimentally infected colony born woodchucks and suggest that viral and/or host factors may influence the site of viral insertion finally detected in overt tumors.

In addition, more than one third (11/28, 39%) tumors with activated N-*myc*2 transcription did not show rearrangement either nearby the gene, or in *b3n* or in *win*. These findings challenge the notion that integration in the downstream *b3n* and *win* loci is responsible for N-*myc*2 activation in tumors lacking insertion nearby N-*myc*2 and suggest that in a considerable fraction of liver tumors, at least from wild woodchucks, N-*myc*2 activation might be due either to WHV integration in further regions of the N-*myc*2 chromosomal domain or to other mechanisms related or unrelated to viral insertion.

Keywords: Hepatocellular carcinoma; Hepadnavirus; Woodchuck hepatitis virus; Hepatitis B virus; Insertional mutagenesis; Oncogene

Introduction

Hepatitis B virus (HBV) chronic infection has long been recognized to be a strong risk factor for development of hepatocellular carcinoma (HCC) (Beasley et al., 1981). The

* Corresponding author. Fax: +39 06 49902662.
E-mail address: rapicett@iss.it (M. Rapicetta).

0042-6822/$ - see front matter © 2005 Elsevier Inc. All rights reserved.
doi:10.1016/j.virol.2005.09.061

Woodchuck hepatitis virus (WHV), another Hepadnavirus closely related to HBV, and its natural host, the woodchuck (*Marmota monax*), are studied as model for HBV infection. WHV is even more oncogenic than HBV, leading to development of hepatocellular carcinoma (HCC) in virtually 100% animals within 1 to 3 years of chronic infection (Popper et al., 1987).

Almost all HCCs from chronically infected individuals harbor one to several clonal integrations of viral DNA (Bréchot et al., 2000). Hepadnavirus integration at specific loci finally observed in overt tumors is thought to occur early in tumor development, according to evidence that random integration and clonal hepatocyte expansion occur in liver tissue both in acute WHV infection (Summers et al., 2003) and in chronic WHV and HBV infection (Mason et al., 2005; Minami et al., 2005).

In woodchuck HCCs, activation of genes of the *myc* family by WHV insertion has been well documented, by far the most frequently affected being N-*myc*2, an intronless retro-transposed version of N-*myc*1. Activation of the N-*myc*2 gene has been shown to result from WHV insertion either nearby the gene (Fourel et al., 1990; Hansen et al., 1993; Wei et al., 1992) or in the *b3n* and *win* downstream loci, located about 10 kb and 150 kb from the gene, respectively (Bruni et al., 1999; Fourel et al., 1994). S/MAR elements detected in *b3n* and *win* might mediate long-range activation of N-*myc*2 by WHV insertion in these loci (Bruni et al., 2004; D'Ugo et al., 1998).

Data about WHV insertion nearby N-*myc*1 or N-*myc*2 in woodchuck liver tumors have been so far reported in four studies (Fourel et al., 1990; Hansen et al., 1993; Jacob et al., 2004; Wei et al., 1992) and in three of them N-*myc*2 transcriptional activation has been analyzed too (Fourel et al., 1990; Hansen et al., 1993; Wei et al., 1992).

Examination of the origin of woodchucks and mode of infection in these four studies shows that data from naturally infected wild woodchucks have been reported only for 5 tumors from 5 animals (Wei et al., 1992): most available data about WHV integrations nearby N-*myc* genes in woodchuck liver tumors were obtained from colony born laboratory bred woodchucks experimentally infected as newborns with standardized viral inocula, mostly of the same lineage (Hansen et al., 1993; Jacob et al., 2004; Wei et al., 1992) and, at lower extent, from woodchucks whose origin and mode of infection were not reported (Fourel et al., 1990). Thus, an unsolved issue is whether or not the observed frequent WHV insertion nearby N-*myc*2 and frequent N-*myc*2 activation in woodchuck HCC may have been influenced by the experimental settings, i.e., the use of standardized viral inocula and colony born woodchucks.

Differently from WHV insertion nearby N-*myc* genes, systematic screening of large HCC surveys for WHV insertions in the *b3n* and *win* loci has not been reported. WHV integration in the *b3n* locus has been so far reported in three individual liver tumors only (Bruni et al., 1995a, 2002; Yamazoe et al., 1991). The *win* locus was identified as a target of WHV integration by analyzing a small group of 13 tumors in which N-*myc*2 transcription was activated in absence of any detectable alteration of the gene (Fourel et al., 1994). Six WHV insertions from 6 tumors were shown to cluster in a 16 kb S*ac*I genomic fragment from *win*.

The discovery of the *b3n* and *win* recurrent targets has led to the notion that WHV insertion in these loci would account for N-*myc*2 activation in those woodchuck liver tumors characterized by active N-*myc*2 transcription in absence of any detectable alteration of the gene, a notion that has remained unproved and not further investigated yet.

In order both to evaluate if this notion is correct and to get more insights into the possible influence of animal origin and mode of infection on frequency of WHV insertion nearby N-*myc*2 and activation of this gene, in the present work, we studied a survey of liver tumors naturally developed in wild woodchucks with naturally acquired chronic WHV infection. In our knowledge, no tumor surveys, either from naturally or from experimentally infected woodchucks, have been so far systematically investigated for N-*myc* activation as well as rearrangement and WHV integration in all known target regions (N-*myc*1, N-*myc*2, *b3n*, and *win*) involved in activation of N-*myc* genes.

Results

Liver tumor nodules were collected at autopsy from 24 wild-caught woodchucks with chronic WHV infection acquired by natural routes. Although a single nodule was observed in 8/24 woodchucks, multifocal HCC largely prevailed, occurring in 16/24 animals. Two, three, and four nodules were observed in 3/24, 3/24, and 6/24 animals, respectively, and more than four nodules (up to 15) in 4/24 animals (Table 1). 70 tumors

Table 1
Woodchucks and liver tumor nodules of the present study

Years of delivery	Woodchuck	Tumors at autopsy	Tumors available
1986	W401/86	1	1
1989	W593/89	1	1
	W594/89	3	1
	W595/89	1	1
	W596/89	2	2
	W598/89	1	1
	W212/89	2	2
1990	W326/90	1	1
1991	W423/91	1	1
	W426/91	1	1
1992	W558/92	4	4
	W596/92	4	4
	W589/92	2	1
1993	W863/93	4	4
	W870/93	4	1
	W891/93	9	9
	W899/93	14	6
1995	W385/95	4	3
	W467/95	4	3
	W477/95	15	7
	W481/95	14	12
1998	W2177/98	3	1
	W2231/98	1	1
	W2234/98	3	2
Total	24	99	70

were available for the present study. Size of collected tumor nodules ranged from 5 mm to 60 mm in diameter, most of them being 10 to 30 mm.

Nodules were confirmed to be HCCs by examination of histological sections of a tumor fragment and adjacent non-tumor liver tissue.

Non-tumor tissue surrounding tumor nodules frequently showed areas of confluent necrosis, while more distal liver parenchyma showed morphological features compatible with a low degree viral infection (mild portal inflammation, occasional lobular activity, rare focal steatosis, mostly of the macrovesicular type) (Fig. 1A). According to previous reports, no evidence of significant fibrosis or cirrhosis was observed in any non-neoplastic samples.

All examined tumor specimens showed similar architecture, mostly of the trabecular type, with similar cytological features: on the whole, they appeared as well-differentiated tumors showing grade 1 features, according to the Edmonson and Steiner (1954) classification (Fig. 1B). No significant hepatocyte polymorphism was observed, except for small focal less well-differentiated areas that could be classified as moderately differentiated focal grade 2 areas (Fig. 1C). On average, cells in focal grade 2 areas were smaller than normal hepatocytes, with rounded and prominent nuclei and, frequently, well visible nucleoli. These cells contained usually little eosinophilic cytoplasm with ill-defined borders. Giant neoplastic cells and significant pleomorphism were only occasionally observed. Mitoses were rare and, usually, with no atypical features; bizarre mitosis were never observed. Vesicles and/or lipid vacuoles were observed in many hepatocytes. Neoplastic tissue was frequently associated to different degrees of necrosis and hemorrhage and, sometimes, to mild inflammation and fibrosis.

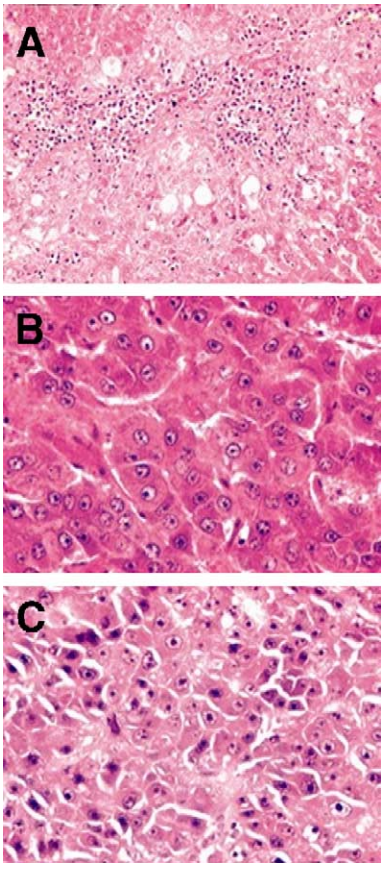

Fig. 1. Photomicrographs of tumor and non-tumor liver sections, stained with hematoxylin–eosin. HCC grading according to Edmonson and Steiner, 1954. Magnification: 250×. (A) Non-neoplastic liver tissue. (B) A well-differentiated HCC, grade 1, showing well-differentiated hepatocytes with normal nuclear to cytoplasm ratio, no significant polymorphism, homogeneous appearance, irregular distribution, and trabecular architecture. (C) A moderately differentiated, grade 2, focal area. Cells still show hepatocyte morphological features, but with appreciable polymorphism and polymorphic size, diffuse distribution, signs of apoptosis and, sometimes, well visible nucleoli and abnormal nuclei.

WHV DNA integration and clonality of liver tumor nodules in multifocal HCCs

A fragment from all 70 tumor tissues as well as a fragment from non-neoplastic liver tissue from each animal were subjected to DNA extraction. WHV DNA integration was evaluated by hybridization with WHV probe of total DNA from tumor and corresponding non-tumor tissues, cleaved with enzymes cutting WHV genome once (H*ind*III, B*gl*II, E*co*RI, S*ac*I). Abundant replicative intermediates were observed in all normal liver samples; remnants of viral replication were also observed in tumor tissues, although at variable but usually lower levels than in normal liver tissue (examples are reported in Fig. 3, in the panels showing hybridization with WHV probe). Detection of hybridizing DNA fragments with size higher than full-length linear 3.3-kb WHV genome with at least two different restriction enzymes was considered evidence for WHV DNA integration.

Comparison of viral integration patterns has been used previously as a molecular marker to establish the possible clonal origin of multiple liver nodules. An identical integration pattern provides evidence for clonal relationships among different nodules.

Nodules from animals showing at least two nodular lesions were analyzed for WHV integration pattern. Analysis of available nodules from animals with up to 4 nodules did not show evidence for clonality; in contrast, evidence for clonal nodules was obtained in three out of four animals showing a number of tumor nodules at autopsy far above the average (W891/93, W477/95, W481/95, harboring 9 to 15 total nodules, see Table 1). In particular, in W891/93 and W477/95, all analyzed nodules (nine and seven nodules, respectively) showed common WHV integration patterns and, thus, were considered to be clonally derived from a primary tumor. In W481/95, only four out of twelve tumors showed a common WHV integration pattern; each of the remaining eight nodules showed independent patterns and was included in the group of independent tumors to be further analyzed.

Based on this analysis, 53 tumors from 24 animals, including one representative tumor of each clonal group, out of 70 analyzed nodules were considered to be independent and further studied.

WHV DNA integration was clearly detected in 48/53 (91%) independent tumors; the presence of integrated WHV DNA could not be established in 2/53 tumors (W596/89-T1 and

W481/95-T10) because of abundant smearing due to viral replicative intermediates (data not shown).

Analysis of tissue DNA for rearrangement and WHV integration in N-myc1, N-myc2, b3n and win loci

All tumor and corresponding non-neoplastic liver DNA samples were analyzed for rearrangement and/or WHV integration in or close to N-*myc*1 and N-*myc*2 genes, as well as in the *b3n* locus; all tumors found to be negative for rearrangements and/or WHV integration in any of these regions but positive for N-*myc*2 transcriptional activation by Northern blotting (see next paragraph), as well as both several randomly chosen samples positive for rearrangement in N-*myc*2 and several randomly chosen samples negative for N-*myc*2 transcription, were also analyzed for rearrangements and/or WHV integration in the *win* locus.

Detection of abnormal fragments in tumor DNA in addition to the fragments observed in non-neoplastic tissue was interpreted as rearrangement of the probed region; if abnormal fragments co-hybridized with the WHV probe, rearrangement was considered to be due to WHV integration.

Fig. 2 reports the partial restriction map of the analyzed regions as well the probes used for hybridization. In order to make our results comparable with data from previous studies, suitable genomic restriction fragments analyzed in previous reports were investigated.

Analysis of N-*myc* genes was previously carried out with different restriction approaches. In two studies, multiple digestions/hybridizations finally resulted in the screening of a −15 kb- to +13-kb genomic region surrounding the N-*myc*2 transcriptional start site (cumulative data from Fourel et al., 1990; Wei et al., 1992); however, all identified N-*myc*2 rearrangements were actually clustered within −3 kb and +3 kb around N-*myc*2 transcriptional start site, i.e., a region included in the B*gl*II genomic fragments from N-*myc*2 analyzed in the subsequent study by Hansen et al. (1993). In Jacob et al. (2004), analysis of N-*myc* genes was carried out by H*in*dIII digestion, likely resulting in underestimation of total N-*myc* rearrangements because excluding an important clustering region of WHV integration located at −3 kb to −2 kb from the 5′ end of N-*myc*2 (Wei et al., 1992; see also Fig. 2A); in addition, it was not assessed if rearrangements involved N-*myc*1 or N-*myc*2.

In order to compare rigorously data from the present study with data from previous reports, all liver and tumor samples from our survey were analyzed for rearrangement of N-*myc* genes both by H*in*dIII digestion (to obtain data comparable with data from Jacob et al., 2004) and by B*gl*II digestion (to obtain data comparable with data from the other studies). In the B*gl*II approach, as in previous studies, it was also determined if rearrangements involved N-*myc*1 or N-*myc*2 and if WHV integrations were 5′ or 3′ with respect to the N-*myc*2 gene.

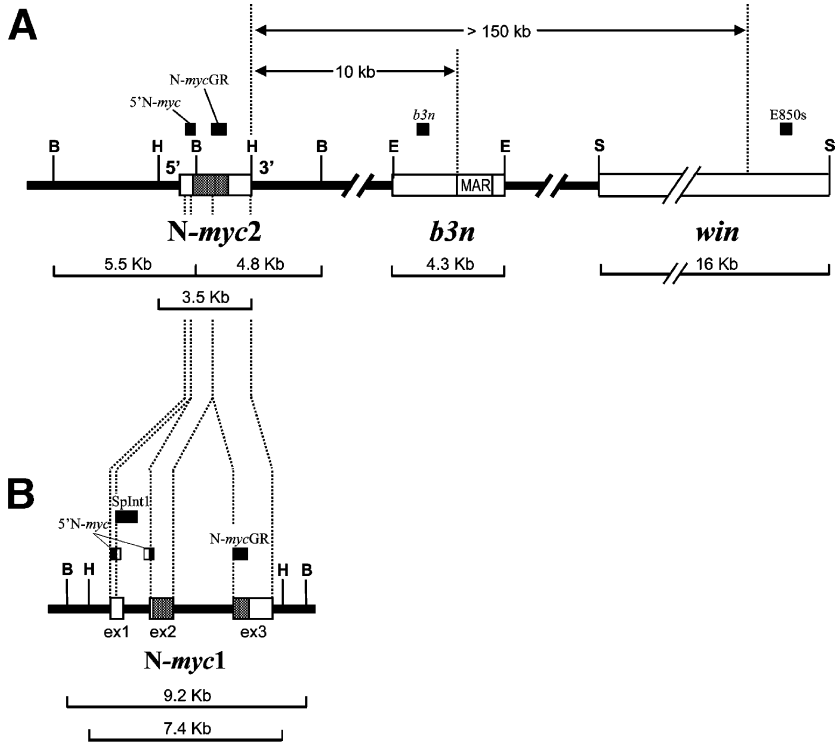

Fig. 2. Partial restriction maps of the N-*myc*2, *b3n*, and *win* regions (A) and N-*myc*1 region (B) analyzed for rearrangement and WHV integration. The probes used in the present study (5′N-*myc*, N-*myc*GR, *b3n*, E850s, SpInt1) are positioned above the corresponding homologous genomic regions. The 5′N-*myc* and N-*myc*GR probes co-hybridize with fragments from both N-*myc*1 and N-*myc*2, although with different affinity because of sequence and structure differences between the two genes. Probe regions completely or strongly homologous with correspondent genomic regions are reported as a black bar, regions with no homology as an open bar. The normal genomic restriction fragments detected by each probe are shown, and their size in kb is indicated. B: BglII; E: E*co*RI; S: S*ac*I. The three N-*myc*1 exons are reported as ex1, ex2, and ex3.

H*ind*III cuts outside of both N-*myc*1 and N-*myc*2 genes, producing a 3.5-kb fragment from N-*myc*2 and a 7.4-kb fragment from N-*myc*1 (Fig. 2). H*ind*III digested DNA was hybridized sequentially with the N-*myc*GR and WHV probes. Fig. 3A reports a representative example of Southern blotting results. Rearranged fragments were detected in W899T1 and W899T2 by the N-*myc*GR probe (Fig. 3A): both fragments co-hybridized with the WHV probe, evidence for WHV insertion nearby N-*myc* genes.

B*gl*II separates the N-*myc*2 gene into two fragments (Fig. 2A): a 5.5-kb fragment, spanning the 5′ end of the gene as well as about 5 kb of upstream DNA, detected by the 5′N-*myc* probe, and a 4.8-kb fragment, spanning most of the coding region as well as the 3′ end, detected by the N-*myc*GR probe. A representative example of Southern blotting analysis of N-*myc* genes by B*gl*II digestion is reported in Fig. 3B. According to hybridization of abnormal fragments to either 5′N-*myc* or N-*myc*GR, WHV integrations and/or rearrangements were mapped to the 5′ or 3′ regions of the N-*myc*2 gene. In the example of Fig. 3B, a rearranged fragment was detected in W899T1 by the 5′N-*myc* probe and in W899T2 by the N-*myc*GR probe; both fragments co-hybridized with the WHV probe. In these tumors, no additional fragments hybridized with the SpInt1 probe, specific for N-*myc*1, proving that rearrangements involved N-*myc*2. Thus, W899T1 and W899T2 harbor WHV integrations located, respectively, 5′ and 3′ of the N-*myc*2 gene.

B*gl*II also produces a unique 9.2-kb fragment containing the entire N-*myc*1 gene (Fig. 2B), detected by both the 5′N-*myc* and the N-*myc*GR probes, as well as by the SpInt1 probe, specific for N-*myc*1. In Fig. 3B, W589TA showed an additional B*gl*II fragment co-hybridizing with 5′N-*myc*, N-*myc*GR, SpInt1, and WHV probes, consistent with a WHV insertion involving N-*myc*1.

The *b3n* region was analyzed by E*co*RI digestion and hybridization first with the *b3n* probe, that detects a 4.3-kb fragment in normal woodchuck liver DNA, according to a previous report (Bruni et al., 1999), and then with the WHV probe. A representative example is shown in Fig. 3C. Rearranged fragments detected inW594T and W899T7 by the *b3n* probe also co-hybridized with the WHV probe, evidence for WHV insertion in the *b3n* locus. Molecular characterization of WHV integrations in these tumors was already reported in detail (Bruni et al., 1995a, 2002). An additional fragment is also visible in W899T4, but it proved to be a partial digestion product because it did not hybridized with the WHV probe and was no more detected by the *b3n* probe in further hybridization experiments (data not shown).

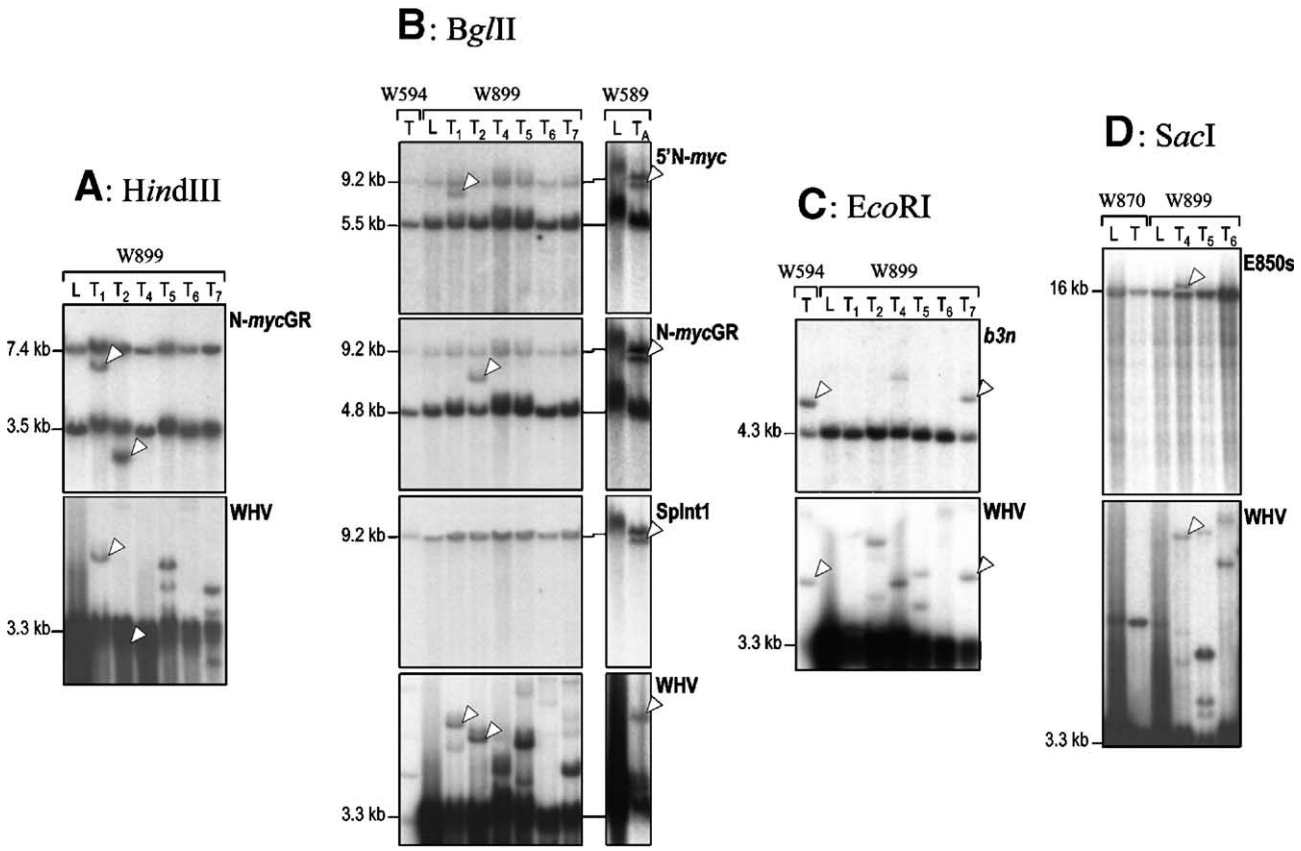

Fig. 3. Southern blotting analysis of total DNA from some liver and tumor tissues for rearrangements and WHV integration in N-*myc* genes (A and B), *b3n* (C) and *win* (D). (A) Hybridization of H*ind*III digested DNA samples from W899/93 with the N-*myc*GR and WHV probes. (B) Hybridization of B*gl*II digested DNA samples from W594/89, W899/93, and W589/92 with the 5′N-*myc*, N-*myc*GR, SpInt1, and WHV probes. (C) Hybridization of E*co*RI digested DNA samples from W594/89 and W899/93 with the *b3n* and WHV probes. (D) Hybridization of S*ac*I digested DNA samples from W870/93 and W899/93 with the E850s and WHV probes. The hybridized probe is reported on the right side of each panel. Open arrowheads show rearranged fragments co-hybridizing with the WHV or other probes. The size (kb) of some reference fragments is reported.

The *win* region was analyzed by S*ac*I digestion and hybridization first with the E850s probe, that detects a 16-kb fragment in normal woodchuck liver DNA, according to a previous report (Fourel et al., 1994), and then with the WHV probe. In the representative example shown in Fig. 3D, a rearranged fragment was detected by E850s probe in W899T4; this fragment co-hybridized with the WHV probe, evidence for WHV insertion in *win*.

Detailed results of Southern analysis of tumors found to be positive for either rearrangement in any of the assayed genomic regions or N-*myc*2 transcriptional activation (see next paragraph) or both are reported in Table 2, together with Northern blotting data. Evidence for rearrangement of N-*myc* genes, with or without WHV insertion, was observed in 20/53 (38%) tumors. N-*myc*1 was found to be an infrequent target of WHV insertion, being involved only in 1/53 tumors (<2%). Rearrangements involved mainly the N-*myc*2 gene and, in most cases, were due to WHV insertion nearby the gene (17/53 tumors, 32%); in nine tumors, viral DNA was located 5′ of the gene and in seven tumors in the 3′ region; in one tumor, it was not possible to establish conclusively the 5′ or 3′ location of viral DNA because results of Southern analysis suggested a complex rearrangement involving viral and cellular sequences (Table 2: W477/95-T). Rearrangement 5′ of N-*myc*2 without WHV insertion was observed in two tumors (Table 2: W863/93-TA and W467/95-T4). Rearrangements of the *b3n* and *win* loci

Table 2
Southern and Northern blotting data of liver tumors positive for either rearrangement in N-*myc*1, N-*myc*2, *b3n* or *win* loci or N-*myc*2 transcriptional activation or both

Woodchuck	Tumors	Additional fragments by Southern blotting[a]						Rearranged locus[b]	N-*myc*2 transcription[a]
		5′N-*myc*	N-*myc*GR		SpInt1	b3n	E850s		
		B*gl*II	H*ind*III	B*gl*II	B*gl*II	E*co*RI	S*ac*I		
W401/86	T	+	+	−	−	−	−	N-*myc*2 (5′)	+ (both 2.3 kb and >2.3 kb)
W212/89	T1	−	+	+	−	−	−	N-*myc*2 (3′)	n.a.
	T2	−	−	−	−	−	+	*win*	n.a.
W594/89	T1	−	−	−	−	+	n.c.	*b3n*	+
W598/89	T	−	+	+	−	−	n.c.	N-*myc*2 (3′)	n.a.
W326/90	T	−	+	+	−	−	n.c.	N-*myc*2 (3′)	+ (>2.3 kb)
W423/91	T	+	+	−	−	−	n.c.	N-*myc*2 (5′)	+
W426/91	TA	−	+	+	−	−	n.c.	N-*myc*2 (3′)	+ (>2.3 kb)
W558/92	T1	−	−	−	−	−	−	None	+
	T2	−	−	−	−	−	−	None	+
	T3	−	−	−	−	−	−	None	+
	T4	−	−	−	−	−	−	None	+
W589/92	TA	+	−	+	+	−	n.c.	N-*myc*1	n.a.
W596/92	T2	+	+	−	−	−	−	N-*myc*2 (5′)	n.a.
W863/93	TA	+[c]	−	−	−	−	−	N-*myc*2 (5′)[d]	+
	TC	+	−	−	−	−	−	N-*myc*2 (5′)	n.a.
	TD	+	−	−	−	−	−	N-*myc*2 (5′)	n.a.
W870/93	TA	−	−	−	−	−	−	None	+
W899/93	T1	+	+	−	−	−	n.c.	N-*myc*2 (5′)	+
	T2	−	+	+	−	−	n.c.	N-*myc*2 (3′)	+ (>2.3 kb)[e]
	T4	−	−	−	−	−	+	*win*	+
	T5	−	−	−	−	−	−	None	+
	T6	−	−	−	−	−	−	None	+
	T7	−	−	−	−	+	n.c.	*b3n*	+
W385/95	T1	−	+	+	−	−	−	N-*myc*2 (3′)	+ (>2.3 kb)
	T2	+	−	−	−	−	−	N-*myc*2 (5′)	+
	T4	−	−	−	−	−	−	None	+
W467/95	T2	+	−	−	−	−	−	N-*myc*2 (5′)	+
	T3	−	−	−	−	−	−	None	+
	T4	+[c]	−	−	−	−	−	N-*myc*2 (5′)[d]	+
W477/95	T	+	+	+	−	−	−	N-*myc*2[f]	+ (>2.3 kb)
W481/95	T2	−	−	−	−	−	−	None	+
	T6	−	−	−	−	−	−	None	+
	T8	+	+	−	−	−	n.c.	N-*myc*2 (5′)	+
W2177/98	T3	−	+	+	−	−	−	N-*myc*2 (3′)	+ (>2.3 kb)[e]

+ and − refer to presence (+) or absence (−) of either additional fragment(s) in Southern blotting or abundant N-*myc*2 transcription in Northern blotting.
n.c.—not carried out.
n.a.—tissue not available for RNA extraction.
[a] All detected additional fragments co-hybridized with the WHV probe, except those marked by [c].
[b] Rearrangements were due to WHV integration, except those marked by [d].
[c] Additional fragments that did not co-hybridized with the WHV probe.
[d] Rearrangement not due to WHV integration.
[e] Transcripts co-hybridizing with the WHV probe.
[f] Unassigned to either 5′ or 3′ because of a complex rearrangement involving viral and cellular sequences.

Table 3
Data about N-*myc* rearrangement and N-*myc*2 activation obtained in the present study compared with data from previous studies

Tumor survey	Infection mode	Animals	Tumors	Tumors with rearrangement in N-*myc* genes			Tumors with N-*myc*2 activation	
				Total	WHV integration only		Total	With WHV integration nearby N-*myc*2
					Nearby N-*myc*1	Nearby N-*myc*2		
Present study	Natural	24	53	20/53 (38%)	1/53 (2%)	17/53 (32%)	28/40 (70%)	12/28 (43%)
Fourel et al., 1990[a]	n.r.	n.r.	30	10/30 (33%)	1/30 (3%)	8/30 (27%)	18/30 (60%)	8/18 (44%)
Wei et al., 1992	Natural	5	5	3/5 (60%)	0/5	3/5 (60%)	4/5 (80%)	3/4 (75%)
	exp.	7	14	10/14 (71%)	0/14	10/14 (71%)	11/14 (79%)	10/11 (91%)
Hansen et al., 1993	exp.	7	17	7/17 (41%)	1/17 (6%)	6/17 (35%)	9/12 (75%)[b]	5/9 (55%)
Jacob et al., 2004	exp.	13	55[c]	23/55 (42%)[d]	21/55 (38%)[d]		n.r.	n.r.
Cumulative data from experimentally infected woodchucks[e]	exp.	14	31	17/31 (55%)	1/31 (3%)	16/31 (52%)	20/26 (77%)	15/20 (75%)

n.r.—not reported.
exp.—experimental.
[a] Some data from this tumor survey were reported in Wei et al., 1992, due to analysis of a further region upstream of N-*myc*2.
[b] Actually, 13 tumors were analyzed for N-*myc* transcription, but 1 tumor showed evidence of extensive RNA degradation and, thus, was not included; in addition, although 10 tumors showed N-*myc* activation, in 1 of them transcripts were most likely from N-*myc*1, because in that tumor WHV integration was demonstrated to involve N-*myc*1, not N-*myc*2 and, thus, was not included in the group of tumors with N-*myc*2 activation.
[c] 51 out of 55 tumors were found to be HCCs, the remaining 4 tumors were adenomas.
[d] Search for N-*myc* rearrangements was carried out by H*ind*III digestion only, limiting analysis to smaller N-*myc* genomic regions than other previous studies and excluding a region upstream of N-*myc*2 shown to be frequently targeted by WHV integration. In addition, the used approach did not distinguish if rearrangements involved N-*myc*1 or N-*myc*2.
[e] Only tumors with both DNA and RNA analysis, cumulative data from Wei et al., 1992 and Hansen et al., 1993.

downstream of N-*myc*2 were found at low frequency (2/53 tumors each locus, 4%) and were caused by WHV insertion in all 4 tumors.

On the whole, rearrangement, with or without WHV insertion, in any known loci of the N-*myc*2 chromosomal domain was observed in 23/53 tumors (43%), and in 21 of them was due to WHV integration.

Data about N-*myc* rearrangement are further summarized and compared to data from previous studies in Table 3.

Analysis of tissue RNA for N-myc transcriptional activation

Enough and suitable tissue was available to analyze RNA too by Northern blotting in 40/53 independent HCCs and corresponding normal liver. A representative example is shown in Fig. 4. N-*myc* transcripts of variable size were detected in all shown tumor samples by the N-*myc*GR probe that detects both N-*myc*1 and N-*myc*2 sequences (Fig. 4A). In tumors W594/89-T, W863/93-TA, W870/93-TA, and W899/93-T1, the 2.3-kb size of the transcript is consistent with the size of the transcription product from the normal promoter of N-*myc*2 gene (Wei et al., 1992). In tumors W326/90-T, W477/95-T1, and W899/93-T2, one or two transcripts with higher size were present. In order to assess if any transcripts, in particular, those ones larger than 2.3 kb, could be N-*myc*1 transcripts or N-*myc*/WHV fusion transcripts or aberrant over-sized N-*myc*2 transcripts, all filters were sequentially hybridized first with the SpInt1 probe, specific for N-*myc*1, and then with the WHV probe. No transcripts hybridized with the SpInt1 probe, specific for N-*myc*1, suggesting that all of them had been produced from N-*myc*2 (data not shown). In W899/93-T2, the N-*myc* transcript co-hybridized with the WHV probe (Fig. 4B), suggesting a WHV/N-*myc*2 fusion transcript. This result was consistent with Southern blotting data, showing in this tumor WHV insertion in the 3′ region of N-*myc*2 (Fig. 3B and Table 2).

Results of Northern blotting analysis of all tumors showing N-*myc*2 activation are included in Table 2. Results are further

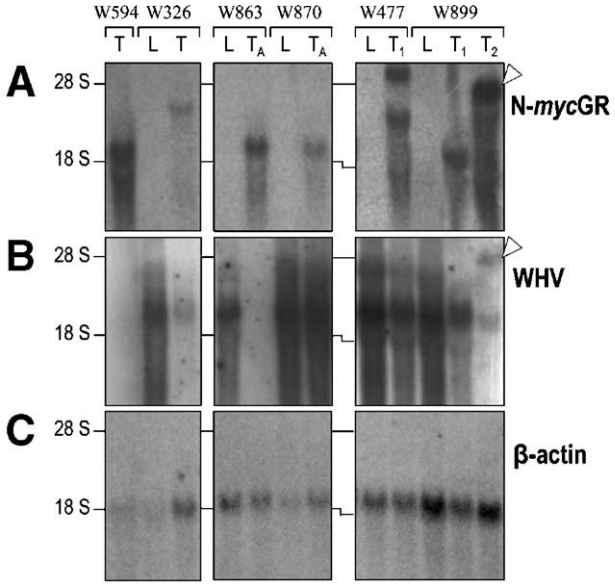

Fig. 4. Northern blotting analysis of total RNA from normal liver and tumor tissues for transcriptional activation of N-*myc* genes. Filters were hybridized sequentially to the N-*myc*GR probe (A), the WHV probe (B) and, finally, the β-actin probe (C) to control for total RNA loading. Open arrowheads indicate transcripts co-hybridizing with both N-*myc*GR and WHV probes. In liver tissues, WHV probe detected high levels of two major transcripts, whose size is consistent with the 3.7 kb and 2.3 kb major viral RNAs previously described in liver tissue of WHV infected woodchucks (Fourel et al., 1990; Buendia, 1992 and references therein); in tumor tissues, the level of these transcripts was highly variable being reduced or absent in some samples and abundant in others.

summarized and compared with data from previous studies in Table 3.

On the whole, abundant N-*myc*2 transcripts were detected in 28/40 (70%) tumors. A single 2.3-kb transcript was detected in 21/28 tumors, while one or two transcripts of heterogeneous size, but exceeding 2.3 kb, were observed in 6/28; one tumor showed both the 2.3 kb and a larger transcript (Table 2: W401/86-T). Co-hybridization with the WHV probe, suggesting WHV/N-*myc*2 fusion transcripts, was observed for transcripts exceeding 2.3 kb from only two tumors (Table 2: W899/93-T2 and W2177/98-T3). These results suggest that transcripts exceeding 2.3 kb detected in the remaining five tumors were more likely products of aberrant transcription, due to either usage of upstream unusual start sites or termination at an alternative downstream site.

Correlation between N-myc2 activation and WHV integration in target regions of N-myc2 chromosomal domain

Transcriptional activation of N-*myc*2 could be related to WHV integration in or close to N-*myc*2, or in *b3n* or in *win* in 12/28 (43%), 2/28 (7%), and 1/28 (<4%) tumors, respectively, while in 2/28 (7%) tumors N-*myc*2 activation was related to rearrangements in the 5′ region of the gene without WHV insertion. Thus, on the whole, N-*myc*2 transcriptional activation was associated to WHV integration and/or rearrangement in known target regions of the N-*myc*2 chromosomal domain in 17/28 (61%) tumors. In the remaining 11/28 (39%) tumors with N-*myc*2 activation, no evidence for WHV insertion or rearrangement in the assayed N-*myc*2, *b3n*, or *win* regions was obtained. The possibility that these results may be due to low or variable sensitivity of Southern blotting/hybridization experiments was excluded because the expected fragments from normal un-rearranged alleles, providing internal control of the entire procedure for each sample, were clearly detected in all tested samples (for an example, see Fig. 3). Remarkably, all tumors with N-*myc*2 activation but no N-*myc*2, *b3n*, and *win* rearrangement had evidence of WHV-DNA integrated somewhere into the host genome, and in all of them, the size of N-*myc*2 transcripts was 2.3 kb as expected for normal transcription from the N-*myc*2 gene (Table 2).

Discussion

According to most previous estimates in both human and woodchuck HCC induced by HBV and WHV, respectively, the great majority of examined tumors of the present study showed evidence of WHV integration into cellular DNA (48/53 tumors, 91%). Although in two tumors WHV integration could not be evaluated, three tumors appeared to be devoid of any detectable viral insertion. It cannot be excluded that in these latter tumors, integrated WHV may be very small, below the detection limit of the Southern blotting/hybridization method because providing a too short target for hybridization. Alternatively, in these tumors, WHV insertion might have been lost during tumor outgrowth because of recombination events, as previously proposed for HBV too.

A careful review of past literature has shown that most data about WHV insertions activating N-*myc* genes in woodchuck liver tumors had been obtained from colony born laboratory bred woodchucks experimentally infected as newborns by standard inocula, mostly of the same lineage (WHV7 or its derivative passage WHV7P1). In a first study, 14 liver tumors had been collected from 7 woodchucks experimentally inoculated with either of two standardized pools of WHV-positive sera (WHV7 and WHV9) (Wei et al., 1992, referring to Popper et al., 1987 for details about experimental infection); in another study, 17 analyzed tumors were collected from 7 woodchucks experimentally infected with the above WHV7 serum pool (Hansen et al., 1993); in a further study, all 55 tumors were obtained from 13 animals inoculated with WHV7P1 (Jacob et al., 2004), an inoculum consisting of serum pooled from four chronic carriers experimentally infected with WHV7 as newborns (Cote et al., 2000).

An aim of the present study was to evaluate the possible influence of animal origin and mode of infection on the frequency of WHV integration nearby N-*myc*2 and transcriptional activation of this gene in woodchuck liver tumors, by comparing our data from naturally infected wild woodchucks with previously published results from experimentally infected colony born animals. A summary of data from present and previous studies is reported in Table 3.

Data from the study by Fourel et al. (1990) were included in Table 3 for completeness but could not be compared with data from wild woodchucks of the present study because mode of infection (natural or experimental) and origin of animals (wild or colony born) were not reported.

As explained in Results section, in the study by Jacob et al. (2004), search for WHV integration in N-*myc* genes was carried out by H*ind*III digestion, thus excluding an important clustering region of WHV integration upstream of the H*ind*III site 5′ of the gene and likely resulting in underestimation of total N-*myc* rearrangements. To carry out rigorous comparison with data from Jacob et al. (2004), we compared data obtained from our tumor survey by the same approach, i.e., H*ind*III digestion (see H*ind*III column in Table 2). The frequency of N-*myc* rearrangements in tumors from wild animals was found to be somewhat lower than in Jacob et al. (2004) (13/53, 25% vs. 23/55, 43%), without reaching, however, statistical significance. We interpreted this result as weakly suggesting that tumors from naturally infected animals may have a lower tendency to harbor WHV integration nearby N-*myc* genes than tumors from experimentally infected animals. Further comparisons were not possible because, due to the aims of their study, Jacob et al. (2004) did not distinguish if N-*myc*1 or N-*myc*2 was involved and, in addition, N-*myc*2 transcription was not analyzed.

The remaining two previous studies reported more abundant data from experimentally infected animals to be compared with our results from wild animals, including N-*myc*2 transcription data (Hansen et al., 1993; Wei et al., 1992). Comparison of data from individual studies gave conflicting results (Table 3): in tumors from our wild animals, the frequencies of (i) total rearrangements in N-myc genes, (ii) WHV integration nearby

N-myc2, and (iii) N-myc2 activation associated to WHV insertion nearby the gene were similar to those reported in Hansen et al. (1993) but showed statistically significant differences with respect to data from Wei et al. (1992). These conflicting results were likely due to random sampling errors because of the small size of the tumor groups from experimentally infected animals. In order to compare our results with as large as possible a tumor group from experimentally infected animals, data from Wei et al. (1992) and Hansen et al. (1993) were combined and reported in Table 3 as a separate row labeled "Cumulative data from experimentally infected animals". Obviously, data from Fourel et al. (1990) and Jacob et al. (2004), for regions described above, could not be included in this group.

As shown in Table 3, in liver tumors from the present study, the N-*myc*1 gene appears to be targeted by WHV insertion at a similar low frequency as in experimentally infected animals (1/53, 2% vs. 1/31, 3%). In contrast, despite a frequency of N-*myc*2 transcriptional activation not substantially different between the two groups (28/40, 70% vs. 20/26, 77%), the frequency of WHV integration nearby N-*myc*2 in naturally infected woodchucks was found to be lower than in experimentally infected animals (17/53, 32% vs. 16/31, 52%), a difference not reaching statistical significance but consistent with the findings from comparison with data from Jacob et al. (2004) (see above), suggesting a tendency of N-*myc*2 activation in wild woodchucks to be less frequently due to WHV integration nearby the gene. Insertions were roughly equally distributed 5′ and 3′ of the N-*myc*2 gene, in contrast with previous studies but without reaching statistical significance.

The above comparisons were carried out between tumor groups including tumors both with and without N-*myc*2 transcriptional activation. In order to better evaluate the possibility that N-*myc*2 activation in wild woodchucks might be less frequently due to WHV integration nearby the gene than in experimentally infected animals, we restricted comparison to only tumors with assessed N-*myc*2 transcriptional activation (last column on the right in Table 3). In this case, WHV insertion nearby the gene was found to be quite lower in our tumor survey than in tumors from experimentally infected animals (12/28, 43% vs. 15/20, 75%), and the difference was statistically significant ($P = 0.0397$ with Fisher's Exact Test).

On the whole, the above comparisons show that some differences indeed exist between tumors from naturally and experimentally infected woodchucks: (i) the frequency of WHV integration nearby N-*myc*2 in tumors from naturally infected animals has a tendency to be lower than in experimentally infected woodchucks, and (ii) in tumors from naturally infected woodchucks, N-*myc*2 activation is due to WHV insertion nearby the gene less frequently than in tumors from experimentally infected animals. We propose that the higher frequencies in experimentally infected animals may be related to the more uniform conditions as to infecting virus and host genetic background and, thus, that viral and/or host factors may influence the site of viral insertion finally detected in liver tumors, possibly by affecting either the integration steps or the post-integration selective processes occurring in the tissue environment during tumor development or both.

The use of standard inocula and colony born laboratory bred animals greatly contributes to reduce experimental variability and to enhance experimental reproducibility of in vivo studies; however, experimental conditions also introduce some bias in biological processes. Indeed, the existence of inoculum-specific biological properties is documented by evidence that inocula of the WHV7 lineage (WHV7 and WHV7P1) exhibit chronicity rates significantly higher than inocula of another lineage (WHV8) (Cote et al., 2000). In addition, the use of colony born laboratory bred animals, even though not inbred, results obviously in animals with a more homogeneous host genetic background than wild animals. These observations provide a rationale and give support to the above proposal.

Another aim of the present study was to evaluate if WHV insertion in the *b3n* and *win* loci would account for N-*myc*2 activation in woodchuck liver tumors actively transcribing N-*myc*2 in absence of any detectable alteration of the gene, as proposed upon discovery of the *b3n* and *win* loci. Since in our tumor survey, we found N-*myc*2 transcriptional activation to be due to WHV integration nearby N-*myc*2 in 43% liver tumors only, we expected frequent WHV integration in the *b3n* and *win* loci in the remaining tumors. In contrast, results showed that the *b3n* and *win* loci were targeted rarely. These findings challenge the notion that N-*myc*2 activation is due to WHV integration either in *b3n* or in *win* in tumors without insertion nearby N-*myc*2. At least in tumors from wild woodchucks, this notion appears to be incorrect: a considerable fraction (39%) of liver tumors with activated N-*myc*2 transcription does not show rearrangement either nearby the N-*myc*2 gene or in the downstream *b3n* and *win* regions. The possibility that N-*myc*2 activation in this latter tumor subgroup might have been induced by exposure to other carcinogenic factors is unlikely because no liver tumors at all were observed in WHV uninfected control woodchucks, reared in the same laboratory environment and delivered each year together with chronically infected animals, evidence for no exposure to further liver carcinogens other than WHV.

In tumors lacking WHV insertion both nearby N-*myc*2 and in the *b3n* and *win* loci, the mechanisms underlying the observed N-*myc*2 activation remain to be determined and several explanations are possible.

Previous observations suggested that N-*myc*2 might be also activated by mechanisms unrelated to WHV integration. N-*myc*2 expression has been detected in nearly all altered hepatic foci (AHFs), considered to be pre-cancerous lesions in woodchuck liver (Yang et al., 1993). In the great majority of AHFs, the N-*myc*2 expression level was somewhat lower than in fully developed HCCs, although a small subset of AHFs was also observed expressing high levels N-*myc*2 transcripts. The estimated high number of N-*myc*2 expressing AHFs per liver (exceeding 1500 per liver) (Yang et al., 1993) favors a hypothesis of underlying mechanism(s) unrelated to WHV integration. Support for this hypothesis has been provided by in vitro studies in human hepatoma cell lines, reporting that the viral X protein (pX) might collaborate with cellular factors to

trans-activate the N-*myc*2 gene (Flajolet et al., 1997). Although authors of this latter study suggested that pX trans-activation might explain the weak N-*myc*2 expression observed at pre-neoplastic stage but not over-expression observed in overt liver tumors, we speculate that mutated aberrant pX versions, as those observed in some HBV related human HCCs (Wang et al., 2004), might show altered properties and play a role as stronger N-*myc*2 trans-activator than wild-type pX in AHFs expressing high levels N-*myc*2 and at least in a fraction of HCCs.

Alternatively, since WHV integration somewhere in cellular DNA was clearly detected in all tumors characterized by N-*myc*2 activation in absence of WHV integration nearby N-*myc*2 and in the *b3n* and *win* loci, WHV integration might activate one or more cellular genes, whose products might be responsible for activating in trans the N-*myc*2 gene.

Finally, a further possibility is that WHV DNA might be inserted at further sites of the N-*myc*2 chromosomal domain, outside the genomic restriction fragments analyzed by Southern blotting, either upstream or downstream of the N-*myc*2 gene and either clustered in additional small regions or scattered along the N-*myc*2 chromosomal domain. Indeed, our current knowledge of the clustered distribution of WHV insertions at defined regions along the N-*myc*2 chromosomal domain in woodchuck liver tumors might also prove to be the result of a combination of both technical limitations of the applied investigation methods and an inherent higher propensity of experimentally infected animals, from which most previous data have been obtained, to develop tumors with activated N-*myc*2 due to WHV integration nearby the gene.

Further studies of the mechanisms underlying activation of N-*myc*2 in woodchuck liver tumors, including the study of the distribution of WHV integrations along the N-*myc*2 chromosomal domain, should help to clarify basic molecular mechanisms, operating in vivo, that could also play a role in activation of cellular genes by HBV integration (Minami et al., 2005; Murakami et al., 2005; Paterlini-Bréchot et al., 2003) in HBV induced human liver cancer too.

Materials and methods

Woodchucks and tissues

All woodchucks (*M. monax*) were wild-caught chronic WHV carriers, whose WHV infection had been acquired by natural routes. They were maintained in isolation in an animal facility at Istituto Superiore di Sanità, Rome, Italy, and received humane care in compliance with the guidelines of the Italian Ministry of Health.

Most woodchucks were purchased from International Animal Exchange Inc. (Ferndale, MI, USA): they were delivered in 1986 (W401/86), in 1989 (W593/89, W594/89, W595/89, W596/89, W598/89, W212/89), in 1990 (W326/90), in 1991 (W423/91, W426/91), in 1992 (W558/92, W596/92, W589/92), in 1993 (W863/93, W870/93, W891/93, W899/93), and in 1995 (W385/95, W467/95, W477/95, W481/95). Three further woodchucks were purchased from North Eastern Wildlife Inc. (South Plymouth, NY, USA) in 1998 (W2177/98, W2231/98, W2234/98).

Plasma was constantly WHV-DNA-positive in all animals, as detected by dot-blot hybridization of follow-up samples, except transient decline to low or undetectable level during short-term antiviral treatments in the frame of studies about anti-HBV drugs in eight woodchucks (W863/93, W870/93, W891/93, W899/93, W385/95, W467/95, W477/95, W481/95) (Fiume et al., 1995, 1997; Zahm et al., 1998). In these studies, fast rebound of viremia at pre-treatment or close to pre-treatment levels was observed in all responding animals when therapy stopped.

One animal (W598/89) was subjected to an experimental super-infection procedure with Hepatitis Delta Virus (HDV) by in vivo liver transfection with a recombinant plasmid containing three head-to-tail cDNA copies of HDV genome. The animal showed evidence of HDV infection (Ciccaglione et al., 1993).

No liver tumor was observed at autopsy in uninfected woodchucks delivered with each group of infected animals and reared in the same laboratory environment.

Liver and tumor tissues were resected at autopsy. Tissue fragments for histological analysis were fixed in 10% buffered formaldehyde, embedded in paraffin, sectioned, and stained. Aliquots of tumor and adjacent non-tumor tissues for DNA and RNA analysis were quickly frozen in liquid nitrogen and stored at −80 °C.

Histopathologic examination of tumor and non-tumor liver tissues

Histologic sections of tumor and non-tumor specimens were stained with hematoxylin–eosin. The tumor histologic grade was determined according to Edmonson–Steiner classification, based on cytological and architectural features (Edmonson and Steiner, 1954).

DNA extraction and Southern blotting

DNA was extracted from non-neoplastic liver and tumor tissues by a previously described procedure, involving incubation of homogenized tissue in the presence of Proteinase K/SDS followed by phenol/chloroform extraction and ethanol precipitation (Bruni et al., 1995a). Purified genomic DNA was digested with restriction enzymes (Roche) according to the manufacturer's instructions. Digested DNA (10 μg) was electrophoresed onto agarose gel, then transferred onto positively charged nylon membrane (Zeta Probe GT, Bio-Rad), according to the manufacturer's instructions.

RNA extraction and Northern blotting

Total RNA was extracted from normal liver and tumor tissues by means of the RNeasy Total RNA Kit (QIAGEN), according to the manufacturer's instructions. Extracted RNA was run in formaldehyde/agarose denaturing gel, then trans-

ferred to nylon filter (Hybond-N, Amersham) by standard procedures (Sambrook et al., 1989).

Labeling and hybridization

Probes were labeled with [α^{32}P]-dCTP with the High Prime DNA labeling kit (Roche) according to the manufacturer's instructions. Filters were hybridized with ^{32}P-labeled probes by standard procedures (Sambrook et al., 1989).

Washing of Southern filters always included a final stringent washing in 0.1 × SSC/0.5% SDS for 30 to 60 min at 65 °C, until decrease of background signals at acceptable levels.

Hybridization of Northern filters was carried out in 50% deionized formamide at 42 °C (Sambrook et al., 1989); after two washings at low stringency, a final stringent washing in 0.2 × SSC, 0.1% SDS at 65 °C for 30 min was carried out.

After autoradiographic film exposure (BioMax MS films, Kodak), filters were stripped and/or allowed to undergo natural decay. Loss of detectable signals was assessed by extended autoradiography exposure before hybridization with a further probe. Co-hybridization of DNA or RNA molecules with multiple probes was assessed by searching for overlapping signals in autoradiographs obtained from the same filter with different probes. In order to identify overlapping signals unambiguously, the faint background images of the whole filter visible after proper exposure as well as reference points visible in all images were exactly aligned.

Probes

Most probes (5′N-*myc*, N-*myc*GR, SpIntI, *b3n* and WHV) were described in detail previously.

The position of N-*myc* probes is schematically reported in Fig. 2; they detect the same H*in*dIII and B*gl*II woodchuck genomic fragments investigated for WHV insertion in previous reports (Fourel et al., 1990; Wei et al., 1992; Hansen et al., 1993; Jacob et al., 2004). The 5′N-*myc* probe spans the 5′ region of N-*myc*2 gene (nucleotides 123 to 466 in the N-*myc*2 sequence Acc. no.X53671) and was amplified by PCR from woodchuck genomic DNA (Bruni et al., 1999) by primers reported previously (Hansen et al., 1993). The N-*myc*GR probe spans the region 1156–1696 in the N-*myc*2 sequence (Bruni et al., 1999). The SpIntI probe is specific for the N-*myc*1 gene because spans one half of exon 1 as well as a fragment of the first intron of N-*myc*1: both regions lack in the N-*myc*2 gene (Fourel et al., 1990); this probe was kindly provided by Dr. M. A. Buendia.

The *b3n* probe spans the region 735 to 1278 of the *b3n* sequence (Acc. no. M60765) (Bruni et al., 1999).

The E850s probe was amplified by PCR with specific primers from the pW1 plasmid, containing a 17-kb insert of the wild-type *win* allele, encompassing the major region of WHV insertion in *win*. pW1 was a kind gift from Dr. M. A. Buendia. The E850s probe spans the region 15358–16173 of the sequenced pW1 insert (Acc. no. AY173019), as confirmed by direct sequencing with the same primers used in PCR. E850s probe includes most of the E850 probe described previously, but is slightly smaller; it detects the same 16-kb S*ac*I fragment from the *win* locus detected by E850 (Fourel et al., 1994).

The WHV probe is a cloned full-length WHV genome and was previously described (Bruni et al., 1995b); it was prepared from the pW8 plasmid, a kind gift from Dr. J. Summers and Dr. J. Pugh.

The β-actin probe was an amplified PCR product from human genomic DNA, and spans a nucleotide region (position 86 to 311 in the human sequence Acc. no. X00351) conserved among human, rat, hamster and mouse (89–93% homology).

Acknowledgments

This work was performed as part of the IRCCS Ospedale Maggiore di Milano and Istituto Superiore di Sanità RF02.188 "Integrated National Project for the Study, the Prevention and the Treatment of the Chronic Hepatology" (n° H95, Experimental Models line) and as part of the Azienda Ospedaliero–Universitaria Pisana/CNR and Istituto Superiore di Sanità "Identification of genomic and proteonomic profiles and new diagnostic and prognostic markers of the outcome of chronic viral hepatitis" project (FIRB art. 8, n° RBNE013PMJ) and was also funded by the project of the Istituto Superiore di Sanità "Viral and Host Factors on Hepatitis Viruses Pathogenesis" (n° C3NC).

We are grateful to M. A. Buendia and G. Fourel for kind gift of the SpInt1 probe and the pW1 plasmid, as well as to have let us gain access to the sequence of the pW1 insert before publication. We are also indebted to J. Summers and J. Pugh for the kind gift of pW8 plasmid and with D. Goletti for the kind gift of human β-actin probe.

We thank Romina Tomasetto and Sabrina Tocchio for the excellent secretarial and editorial assistance, Armando Cesolini for the careful animal care, and Roberto Gilardi and Walter Tranquilli for the graphic elaboration.

References

Beasley, R.P., Lin, C.C., Hwang, L.Y., Chien, C.S., 1981. Hepatocellular carcinoma and hepatitis B virus. Lancet 2, 1129–1133.

Bréchot, C., Gozuacik, D., Murakami, Y., Paterlini-Bréchot, P., 2000. Molecular bases for the development of hepatitis B virus (HBV)-related hepatocellular carcinoma (HCC). Semin. Cancer Biol. 10, 211–231.

Bruni, R., Argentini, C., D'Ugo, E., Giuseppetti, R., Ciccaglione, A.R., Rapicetta, M., 1995a. Recurrence of WHV integration in the b3n locus in woodchuck hepatocellular carcinoma. Virology 214, 229–234.

Bruni, R., Argentini, C., D'Ugo, E., Giuseppetti, R., Rapicetta, M., 1995b. A PCR based strategy for mapping of Hepadnavirus integrated sequences in hepatocellular carcinomas. J. Virol. Methods 52, 347–360.

Bruni, R., D'Ugo, E., Giuseppetti, R., Argentini, C., Rapicetta, M., 1999. Activation of the N-myc2 oncogene by Woodchuck hepatitis virus integration in the linked downstream b3n locus in woodchuck hepatocellular carcinoma. Virology 257, 483–490.

Bruni, R., Villano, U., D'Ugo, E., Giuseppetti, R., Argentini, C., Rapicetta, M., 2002. Induction of oncogene activation by hepatitis B virus integration affecting key genome regulative elements: evidence from the Woodchuck hepatitis virus/woodchuck model. In: Margolis, H.S., Alter, M.J., Liang, T.J., Dienstag, J.L. (Eds.), Viral Hepatitis and Liver Disease. Proceedings Book of the 10th International Symposium on Viral Hepatitis and Liver Disease. International Medical Press, London, pp. 432–437.

Bruni, R., D'Ugo, E., Villano, U., Fourel, G., Buendia, M.A., Rapicetta, M.,

2004. S/MAR elements in the *win* locus targeted by WHV integration in woodchuck liver tumors. Virology 329, 1–10.

Buendia, M.A., 1992. Hepatitis B viruses and hepatocellular carcinoma. Adv. Cancer Res. 59, 167–226.

Ciccaglione, A.R., Rapicetta, M., Fabiano, A., Argentini, C., Silvestro, M., Giuseppetti, R., Varano, F., D'Urso, N., Dinolfo, L., Morgando, A., Bruni, R., Ponzetto, A., 1993. Chronic infection in woodchucks infected by a cloned hepatitis delta virus. Arch. Virol. 8, 15–21.

Cote, P.J., Korba, B.E., Miller, R.H., Jacob, J.R., Baldwin, B.H., Hornbuckle, W.E., Purcell, R.H., Tennant, B.C., Gerin, J.L., 2000. Effects of age and viral determinants on chronicity as an outcome of experimental Woodchuck hepatitis virus infection. Hepatology 31, 190–200.

D'Ugo, E., Bruni, R., Argentini, C., Giuseppetti, R., Rapicetta, M., 1998. Identification of Scaffold/Matrix attachment region in recurrent site of Woodchuck hepatitis virus integration. DNA Cell. Biol. 17, 519–527.

Edmonson, H.A., Steiner, P.E., 1954. Primary carcinomas of the liver. A study of 100 cases among 48,900 necropsies. Cancer 7, 462–503.

Fiume, L., Di Stefano, G., Busi, C., Mattioli, A., Rapicetta, M., Giuseppetti, R., Ciccaglione, A.R., Argentini, C., 1995. Inhibition of Woodchuck hepatitis virus replication by adenine arabinoside monophosphate coupled to lactosaminated poly-L-lysine and administered by intramuscular route. Hepatology 22, 1072–1077.

Fiume, L., Di Stefano, G., Busi, C., Mattioli, A., Gervasi, G.B., Bestini, M., Batoli, C., Catalani, R., Caccia, G., Farina, C., Fissi, A., Pieroni, O., Giuseppetti, R., D'Ugo, E., Bruni, R., Rapicetta, M., 1997. Hepatotropic conjugate of adenine arabinoside monophosphate with lactosaminated poly-L-lysine. Synthesis of the carrier and pharmacological properties of the conjugate. J. Hepatol. 26, 253–259.

Flajolet, M., Gegonne, A., Ghysdael, J., Tiollais, P., Buendia, M.A., Fourel, G., 1997. Cellular and viral transacting factors modulate N-myc2 promoter activity in woodchuck liver tumors. Oncogene 15, 1103–1110.

Fourel, G., Trepo, C., Bougueleret, L., Henglein, B., Ponzetto, A., Tiollais, P., Buendia, M.A., 1990. Frequent activation of N-myc genes by Hepadnavirus insertion in woodchuck liver tumors. Nature 347, 294–298.

Fourel, G., Couturier, J., Wei, Y., Apiou, F., Tiollais, P., Buendia, M.A., 1994. Evidence for long-range oncogene activation by Hepadnavirus insertion. EMBO J. 13, 2526–2534.

Hansen, L.J., Tennant, B.C., Seeger, C., Ganem, D., 1993. Differential activation of *myc* gene family members in hepatic carcinogenesis by closely related hepatitis B viruses. Mol. Cell. Biol. 13, 659–667.

Jacob, J.R., Sterczer, A., Toshkov, I.A., Yeager, A.E., Korba, B.E., Cote, P.J., Buendia, M.A., Gerin, J.L., Tennant, B.C., 2004. Integration of woodchuck hepatitis and N-myc rearrangement determine size and histologic grade of hepatic tumors. Hepatology 39, 1008–1016.

Mason, W.S., Jilbert, A.R., Summers, J., 2005. Clonal expansion of hepatocytes during chronic Woodchuck hepatitis virus infection. Proc. Natl. Acad. Sci. U.S.A. 25 (102), 1139–1144.

Minami, M., Daimon, Y., Mori, K., Takashima, H., Nakajima, T., Itoh, Y., Okanoue, T., 2005. Hepatitis B virus-related insertional mutagenesis in chronic hepatitis B patients as an early drastic genetic change leading to hepatocarcinogenesis. Oncogene 24, 4340–4348.

Murakami, Y., Saigo, K., Takashima, H., Minami, M., Okanoue, T., Bréchot, C., Paterlini-Bréchot, P., 2005. Large scaled analysis of hepatitis B virus (HBV) DNA integration in HBV related hepatocellular carcinomas. Gut 54, 1162–1168.

Paterlini-Bréchot, P., Saigo, K., Murakami, Y., Chami, M., Gozuacik, D., Mugnier, C., Lagorce, D., Bréchot, C., 2003. Hepatitis B virus-related insertional mutagenesis occurs frequently in human liver cancers and recurrently targets human telomerase gene. Oncogene 22, 3911–3916.

Popper, H., Roth, L., Purcell, R.H., Tennant, B.C., Gerin, J.L., 1987. Hepatocarcinogenicity of the Woodchuck hepatitis virus. Proc. Natl. Acad. Sci. U.S.A. 84, 866–870.

Sambrook, J., Fritsch, E.F., Maniatis, T., 1989. Molecular Cloning. A Laboratory Manual, 2nd ed. Cold Spring Harbor Laboratory Press, Cold Spring Harbor, N.Y.

Summers, J., Jilbert, A.R., Yang, W., Aldrich, C.E., Saputelli, J., Litwin, S., Toll, E., Mason, W.S., 2003. Hepatocyte turnover during resolution of a transient hepadnaviral infection. Proc. Natl. Acad. Sci. U.S.A. 100, 11652–11659.

Wang, Y., Lau, S.H., Sham, J.S., Wu, M.C., Wang, T., Guan, X.Y., 2004. Characterization of HBV integrants in 14 hepatocellular carcinomas: association of truncated X gene and hepatocellular carcinogenesis. Oncogene 23, 142–148.

Wei, Y., Fourel, G., Ponzetto, A., Silvestro, M., Tiollais, P., Buendia, M.A., 1992. Hepadnavirus integration: mechanisms of activation of the N-myc2 retrotransposon in woodchuck liver tumors. J. Virol. 6, 5265–5276.

Yamazoe, M., Nakai, S., Ogasawara, N., Yoshikawa, H., 1991. Integration of woodchuck hepatitis virus (WHV)-DNA at two chromosomal sites (V_k and *gag*-like) in a hepatocellular carcinoma. Gene 100, 139–146.

Yang, D., Alt, E., Rogler, C.E., 1993. Coordinate expression of N-*myc*2 and insulin-like growth factor II in precancerous altered hepatic foci in Woodchuck hepatitis virus carriers. Cancer Res. 53, 2020–2027.

Zahm, F.E., Bonino, F., Giuseppetti, R., Rapicetta, M., 1998. Antiviral activity of ganciclovir, 9-(1,3-dihydroxy-2-propoxymethyl) guanine against Woodchuck hepatitis virus: quantitative measurement of Woodchuck hepatitis virus DNA using storage phosphor technology. Ital. J. Gastroenterol. Hepatol. 30, 510–516.